

ENaC gene variants and their involvement in Covid-19 severity

ELENI KONIARI¹, KYRIAKI HATZIAGAPIOU^{1,2}, ALEXANDRA OLTI NIKOLA², KONSTANTINA GEORGOULIA¹,
NIKOLAOS MARINAKIS³, PETROS BAKAKOS⁴, ATHANASIA ATHANASOPOULOU⁴,
ATHANASIOS KOROMILIAS⁴, NIKOLETTA ROVINA⁴, VASILIKI EFTHYMIU¹, ELENI PAPAKONSTANTINO⁵,
DIMITRIOS VLACHAKIS⁵, SOPHIA MAVRIKOU⁶, ANTONIA KOUTSOUKOU⁴,
JOANNE TRAEGER-SYNODINOS³ and GEORGE P. CHROUSOS¹

¹University Research Institute of Maternal and Child Health and Precision Medicine and UNESCO Chair on Adolescent Health Care, National and Kapodistrian University of Athens, 11527 Athens, Greece; ²First Department of Pediatrics, National and Kapodistrian University of Athens, 'Aghia Sophia' Children's Hospital, 11527 Athens, Greece; ³Laboratory of Medical Genetics, St. Sophia's Children's Hospital, Medical School, National and Kapodistrian University of Athens, 11527 Athens, Greece; ⁴Intensive Care Unit, First Department of Pulmonary Medicine, National and Kapodistrian University of Athens and Sotiria Hospital, 11527 Athens, Greece; ⁵Laboratory of Genetics, Department of Biotechnology, School of Applied Biology and Biotechnology, Agricultural University of Athens, 10447 Athens, Greece; ⁶Faculty of Applied Biology and Biotechnology, Department of Biotechnology, Agricultural University of Athens, 10447 Athens, Greece

Received April 19, 2024; Accepted August 5, 2024

DOI: 10.3892/br.2024.1864

Abstract. Epidemiological studies report the association of diverse cardiovascular conditions with coronavirus disease 2019 (COVID-19), but the causality has remained to be established. Specific genetic factors and the extent to which they can explain variation in susceptibility or severity are largely elusive. The present study aimed to evaluate the link between 32 cardio-metabolic traits and COVID-19. A total of 60 participants were enrolled, who were categorized into the following 4 groups: A control group with no COVID-19 or any other underlying pathologies, a group of patients with a certain form of dyslipidemia and predisposition to atherosclerotic disease, a COVID-19 group with mild or no symptoms and a COVID-19 group with severe symptomatology hospitalized at the Intensive Care Unit of Sotiria Hospital (Athens, Greece). Demographic, clinical and laboratory data were recorded and genetic material was isolated, followed by simultaneous analysis of the genes related to dyslipidemia using a custom-made next-generation sequencing panel. In the COVID-19 group with mild or absent symptoms, the variant c.112C>T:p.P38S was detected in the

sodium channel epithelial 1 subunit α (SCNN1A) gene, with a major allele frequency (Maf) of <0.01. In the COVID-19 group with severe symptoms, the variant c.786G>A:p.T262T was detected in the SCNN1B gene, which encodes for the β -subunit of the epithelial sodium channel ENaC, with a Maf <0.01. None of the two rare variants were detected in the control or dyslipidemia groups. In conclusion, the current study suggests that ENaC variants are likely associated with genetic susceptibility to COVID-19, supporting the rationale for the risk and protective genetic factors for the morbidity and mortality of COVID-19.

Introduction

Severe Acute Respiratory Syndrome Coronavirus-2 (SARS-CoV-2) is a coronavirus-related disease that has been spreading globally since December 2019. The disease is known as Coronavirus disease 2019 (COVID-19) and its clinical spectrum varies significantly from asymptomatic or mild, common cold- or influenza-like disease to a more severe lower respiratory tract illness, associated with acute respiratory distress syndrome, pulmonary failure, septic shock and/or multiple organ dysfunction (1,2). Various underlying comorbidities are considered risk factors for progression to severe COVID-19. Thus, authoritative agencies, such as the US and European Centers for Disease Control and Prevention have issued warnings for several factors, which may contribute to severe outcomes in at-risk populations, e.g. aged ≥ 65 years old, diabetes type 1 or type 2 diabetes mellitus, obesity (body mass index ≥ 35 kg/m²), pregnancy, cancer, primary or acquired immunodeficiency/immunosuppression, chronic tobacco smokers and haemoglobinopathies, as well as cardiovascular, pulmonary, chronic kidney and liver disease. However, there are also patients with no apparent co-morbidities who

Correspondence to: Dr Eleni Koniari, University Research Institute of Maternal and Child Health and Precision Medicine and UNESCO Chair on Adolescent Health Care, National and Kapodistrian University of Athens, Thivon and Livadias Str. 8, 11527 Athens, Greece
E-mail: hkoniari@med.uoa.gr

Key words: dyslipidemia, genetics, ENaC, SARS-Cov2, atherosclerosis

eventually develop severe SARS-CoV-2 infection with poor outcomes (1).

Dyslipidemia is an established risk factor for severe COVID-19 infection, due to several reasons. Primarily, patients with dyslipidemia may have high levels of low-density lipoprotein (LDL). The latter interacts with macrophages in atherosclerotic plaques, leading to increased inflammatory gene expression (3). Furthermore, excess LDL accumulation in macrophage cells results in cholesterol crystal deposition, leading to inflammasome activation and the secretion of proinflammatory cytokines, such as IL-1 β and IL-18. However, the presence of high levels of pro-inflammatory cytokines has been linked with severe outcomes via the 'cytokine release syndrome', characterized by systemic inflammation and multiorgan dysfunction (4). Furthermore, patients with dyslipidemia may also have low levels of high-density lipoprotein (HDL). This fraction itself is involved in the regulation of the innate immune response. HDL down regulates T-cell activation and inflammatory mediators' expression in macrophages and dendritic cells, via interaction with ATP-binding cassette protein A1 (ABCA1) or ABCG1. HDL levels in the acute phase of coronavirus infection have also been associated with disease activity, as a decrease in the number of small HDL particles is inversely associated with the disease activity score and C-reactive protein levels (5). The aforementioned alterations contribute to the dysregulation of the innate immune response, the first-line defense against any invading pathogens (6). In patients with dyslipidemia, the accumulation of LDL and triglycerides may cause additional endothelial dysfunction (7). The latter is accentuated during COVID-19 infections, as the SARS-CoV-2 receptor angiotensin 2-converting enzyme (ACE2) is also expressed by endothelial cells (8). The combination of these risk factors leads to the development of cardiovascular complications associated with severe clinical outcomes. Beyond innate immunity, dyslipidemia is also a critical regulator of adaptive immunity, as it has an impact on the differentiation and function of CD4+ T cells, CD8+T cells and B-cells (9).

The lipid profiles of patients with COVID-19 are quite variable (10,11). A likely explanation is that the genetics and epigenetics of dyslipidemia and other pathologic states may differ among patients with COVID-19. In the context of the growing need to understand the pathogenic mechanisms of this aggressive RNA virus and its relation to dyslipidemia and other cardiovascular traits, the present study aimed to analyze a comprehensive panel of specific genes involved in cardio-pulmonary, metabolic and vascular disorders associated with COVID-19.

Materials and methods

Subjects and genetic analysis. In the present study, 60 consecutive cases were enrolled retrospectively (2019-2021) divided into four groups, i.e.: i) The control group, volunteers who came for a regular check up (n=14), with an age range of 28-69 years (43% men and 57% women; none of the subjects in this group had COVID-19 or any other underlying pathologies); ii) adult patients (visiting the Lipid Outpatient Departments through convenience sampling) with a type of dyslipidemia and predisposition to atherosclerotic disease (n=18), with an

age range of 10-56 years (72% men and 28% women), and none of the subjects in this group had COVID-19; iii) patients with COVID-19 and mild or no symptoms (L/NO S) (n=16) with an age range of 22-67 years (38% men and 62% women); iv) patients with COVID-19, who were hospitalized with severe COVID-19 symptoms in the Intensive Care Unit (ICU) of Sotiria Hospital (Athens, Greece) (n=12) with an age range of 39-91 years (50% men and 50% women). The collection of samples was performed by the University Research Institute of Maternal and Child Health and Precision Medicine, National and Kapodistrian University of Athens, in collaboration with the ICU of Sotiria Thoracic Diseases Hospital (Athens, Greece). All patients or their representatives/relatives consented to their participation in the study.

Demographic, clinical and laboratory data were recorded, blood was obtained by venipuncture and genetic material was isolated (NucleoSpin Blood; Macherey Nagel), followed by simultaneous analysis of the genes low density lipoprotein receptor (LDLR), apolipoprotein B-100 (APOB-100), proprotein convertase subtilisin/kexin type 9, lipoprotein (LP)- α , angiotensin-like 3 gene, APOB, microsomal triglyceride transfer protein, secretion associated, Ras related GTPase 1B, ATP-binding cassette (ABC) transporters G5 (ABCG5), angiotensin II type I receptor (AGTR1), 11- β -hydroxysteroid dehydrogenase type 2, epithelial sodium channel (EnaC), inducible nitric oxide synthases chromosome 17 (NOS2), APOE, LP lipase, APOA5, APOC3, cholesteryl ester transfer protein, scavenger receptor class B type 1, phospholipid transfer protein, NPC intracellular cholesterol transporter 1 (NPC1), NPC2 (NIEMANN-Pick C), sphingomyelin phosphodiesterase 1 (SMPD1), fat mass and obesity-associated gene (FTO), dual specificity tyrosine phosphorylation regulated kinase 1B, melanocortin 4 receptor and chymase 1, using a custom-made next-generation sequencing panel, designed by the correspondent author and manufactured by SOPHiA GENETICS. The exon and adjacent intrinsic/exon regions of the above-mentioned genes were sequenced on the Illumina MiSeq platform (Illumina, Inc.), followed by bioinformatics analyses of the sequencing files from the validated platform of the company Sophia Genetics DDM and the Varaft annotation tool (<https://bio.tools/varaft>).

Statistical analysis. Values are expressed as the mean and standard deviation or the median and interquartile range. Differences between independent samples were assessed with Student's t-test or the Mann-Whitney U-test considering the assumption of normality, which was checked through kurtosis, skewness and the Shapiro-Wilk test. Statistical analysis was performed using SPSS version 26.0 (IBM Corp). $P \leq 0.05$ was considered to indicate a statistically significant difference.

Results

Patient data. In the current study, 60 participants were included, divided into four groups, i.e. i) The non-Covid Control group, ii) non-Covid dyslipidemic patients, iii) Covid-19 L/NO symptoms group, and iv) the Covid-19 ICU group. Available demographic data and biomedical parameters are shown in Tables I and II. The median age was significantly different among the four groups (non-Covid

Table I. Demographic data.

Item	Control (n=14)	Dyslipidemic (n=18)	Covid-ICU (n=12)	Covid-L/NO S (n=16)	P-value
Gender					0.189 ^a
Female	8 (57)	5 (28)	6 (50)	10 (62)	
Male	6 (43)	13 (72)	6 (50)	6 (38)	
Age, years					<0.001 ^b
Range	26-72	8-66	39-91	21-54	
Mean	44	22	28	40	
Median	49	36	65	38	
Ethnicity					0.485 ^c
Greek (Caucasians)	14	16 (89)	11 (92)	16 (100)	
Other	-	2 (11)	1 (8)	-	

^aChi-square test, ^banalysis of variance, ^cMonte Carlo simulation. Values are expressed as n (%). ICU, intensive care unit; L/NO S, L/NO S, low or no symptomatology. Differences in age were found between controls vs. dyslipidemic and Covid-L/NO, dyslipidemic vs. Covid-ICU and Covid-L/NO, Covid-ICU vs. Covid-L/NO group.

Table II. Differences in laboratory parameters between Group 4 (ICU) vs. Group 3 (L/NO S).

Parameter (normal range)	ICU	L/NO S	P-value
HCT, % (females, 37-47; males, 42-50)	38.30 (3.80)	41.00 (3.00)	0.030
PLTs, K/ μ l (152-433)	190.50 (146.50)	236.00 (57.00)	0.235
INR	1.15 \pm 0.19	0.95 \pm 0.07	0.204
PT, sec (11-13)	14.20 (1.60)	19.45 (18.30)	>0.999
CRP, mg/dl (low risk, <0.1; average risk, 0.1-0.3; high risk, >0.3)	6.85 (7.06)	2.70 (1.70)	0.019
GLU, mg/dl (70-99)	197.10 \pm 86.27	94.31 \pm 9.95	0.004
CREA, mg/dl (female: 0.5-1.1; male: 0.70-1.30)	0.77 \pm 0.23	0.91 \pm 0.15	0.091
SGOT, IU/l (10-48)	50.00 (45.00)	18.00 (9.00)	0.001
SGPT, IU/l (10-40)	57.00 (65.00)	19.00 (7.00)	<0.001
γ -GT, IU/l (females, 8-40; males, 9-50)	77.00 (156.00)	19.00 (9.00)	<0.001
K, mmol/l (3.5-5.0)	4.08 \pm 0.40	4.41 \pm 0.34	0.044
Na, mmol/l (136-145)	138.00 (4.00)	143.00 (5.00)	0.042
TBIL, mg/dl (0.3-1.0)	0.73 \pm 0.34	1.19 \pm 0.79	0.333
Ferr, ng/ml (females, 24-307; males, 24-336)	498.00 (889.90)	48.00 (22.00)	<0.001
TC, mg/dl (<200)	129.82 \pm 28.33	215.38 \pm 46.01	<0.001
LDL, mg/dl (<100)	75.45 \pm 23.14	133.46 \pm 36.49	<0.001
HDL, mg/dl (females, >50; males, >40 mg/dl)	33.00 (12.00)	55.00 (10.00)	0.001

Values are expressed as the mean \pm standard deviation (comparison performed using the T-test or median (interquartile range) (comparison with the Mann-Whitney U-test). HCT, hematocrit; PTLs, platelets; INR, international normalized ratio; PT, prothrombin time; CRP, C-reactive protein; GLU, glucose; CREA, creatinine; SGOT, serum glutamic-oxaloacetic transaminase; SGPT, serum glutamic-pyruvic transaminase; γ -GT, γ -glutamyl transferase; K, potassium; Na, sodium; Cl, chloride; TBIL, total bilirubin; Ferr, ferritin; TC, total cholesterol; LDL, low-density lipoprotein cholesterol; HDL, high-density lipoprotein cholesterol; TG, triglycerides; ICU, intensive care units; L/NO S, low or no symptomatology.

Controls vs. non-Covid dyslipid and ICU, non-Covid dyslipid vs. Controls, L/NO and ICU, L/NO vs. dyslipid and ICU, ICU vs. non-Covid Controls, non-Covid dyslipid and L/NO; P<0.001), but there were no significant differences in gender. Glucose levels, serum glutamic-oxaloacetic transaminase, serum glutamic-pyruvic transaminase and γ -glutamyl transferase levels were significantly higher in the ICU group

compared to the L/NO S group (P<0.05). Of note, total cholesterol (TC) and LDL cholesterol levels were lower in the ICU group compared with the L/NO S group, whereas triglycerides (TGs) were higher.

Genetic analysis. None of the subjects in Group 1 (control) had a mutation or pathogenic variant in the studied genes.

Table III. Variants detected in the four study groups.

A, Group 1: Control						
Gene	AA change	FREQ HET/ 500	FREQ HOM/ 500	SNP 150	UMD prediction	Gnomad
PCSK9 NM_174936	Exon5:c.709C>T:p.R237W	0	0	rs148195424	US	0.0007
APOB NM_000384	Exon29:c.12382G>A:p.V4128M	6	0	rs1801703	P	0.0063
	Exon26:c.10131G>A:p.L3377L	6	0	rs1799812	P	0.0063
	Exon26:c.9075delA:p.L3025fs	0	0	-	NA	-
	Exon26:c.4449A>G:p.E1483E	2	0	rs151018874	P	0.0022
	Exon22:c.3337G>C:p.D1113H	16	1	rs12713844	P	0.0068
B, Group 2: Dyslipidemic						
Gene	AA change	FREQ HET/ 500	FREQ HOM/ 500	Av SNP 150	UMD prediction	Gnomad (P-values)
AGTR1 NM_009585	exon2:c.30T>C:p.G10G	0	0	rs747843312	FH	0
APOB NM_000384	exon26:c.11354C>T:p.T3785I	2	0	rs143710616	-	0
	exon26:c.5652C>T:p.N1884N	0	0	rs766106302	-	0
	exon22:c.3426G>A:p.S1142S	1	0	rs142448733	FH/HYP	0.0005
	exon9:c.1088T>C:p.V363A	1	0	rs751259935	-	0
	exon16:c.2412C>T:p.R804R	0	0	rs755974543	-	0
FTO NM_001363897	exon3:c.778G>T:p.A260S	0	0	-	-	-
LMF1 NM_001352018	exon4:c.115+1G>A	3	0	rs72759474	-	0.0011
LDLR NM_001195799	exon3:c.394T>C:p.C132R	0	0	rs879254558	FH	-
	exon4:c.354C>A:p.S118R	1	0	rs140241383	FH	0
	exon7:r.spl	3	-	-	-	-
	exon9:c.1142G>A:p.G381D	0	0	rs28941776	FH	0
	exon12:c.1706-10G>A	15	0	rs17248882	FH	0.0002
	exon12:c.1550C>T:p.P517L	0	0	rs28942084	FH	0.00616
LMF1 NM_001352019	exon9:c.964G>A:p.A322T	0	0	rs186247027	-	0
	exon8:c.758T>G:p.V253G	0	0	rs368408082	-	0
LPA NM_005577	exon16:c.2490T>C:p.N830N	0	0	-	-	0
	exon8:c.1161T>A:p.T387T	27	1	rs4709450	-	0.0222
	exon8:c.1122T>C:p.N374N	0	0	-	-	0
MTTP NM_001300785	exon17:c.2514G>C:p.L838F	0	0	rs144590904	ABETA	0.0004
	exon26:c.3173A>G:p.D1058G	0	0	rs371929273	-	0
NOS2 NM_000625	exon3:c.135G>A:p.Q45Q	2	0	rs201239372	-	0
PLTP NM_000625	exon7:c.447G>A:p.R149R	6	0	rs141035863	-	0.0002
SAR1b NM_016103	NM_016103:exon6:c.480+3A>-	1	0	-	-	-
SCARB1 NM_001367987	exon10:c.1243G>A:p.G415R	6	0	rs144985120	-	0
SCNN1A NM_001159576	exon5:c.1250A>G:p.E417G	0	0	rs569195112	PHA	0
	exon1:c.111G>A:p.P37P	2	0	rs573341191	-	0
SCNN1B NM_000336	exon2:c.245C>G:p.S82C	6	6	rs35731153	BR	0.0012
	exon13:c.1782G>A:p.T594T	2	0	rs13306628	PYA	0.0002
SCNN1D NM_001130413	exon3:c.129G>T:p.L43L	0	0	rs778315388	-	0
	exon5:c.450G>C:p.G150G	3	0	rs199854533	-	0
	exon12:c.1621G>C:p.V541L	3	0	rs202246275	-	0.001
SMPD1 NM_000543	exon2:c.729C>T:p.A243A	0	0	rs149476159	SCL	0

Table III. Continued.

C, Group 3: COVID-19 (L/NO S)

Gene	AA change	FREQ HET/500	FREQ HOM/500	Av SNP 150	UMD prediction	Gnomad (P-values)
APOB NM_000384	exon29:c.12382G>A:p.V4128M	6	0	rs1801703	P	0.0063
	exon26:c.10131G>A:p.L3377L	6	0	rs1799812	P	0.0063
	exon26:c.9321C>T:p.N3107N	0	0	rs72653101	P	0.0001
	exon26:c.4825T>C:p.L1609L	1	0	rs72653083	P	0.0019
	exon22:c.3383G>A:p.R1128H	0	0	rs12713843	P	0.0041
	exon22:c.3337G>C:p.D1113H	16	1	rs12713844	P	0.0068
	exon16:c.2258G>A:p.G753E	2	0	rs148502464	P	0.0002
SCNN1A NM_001038	exon2: c.112C> T: p.P38S	0	0	-	-	-

D, Group 4: COVID-19 (ICU)

Gene	AA change	FREQ HET/500	FREQ HOM/500	Av SNP 150	UMD prediction	Gnomad (P-values)
APOB NM_000384	exon26:c.9736T>C:p.F3246L	0	0	-	PP	-
	exon26:c.9294C>T:p.Y3098Y	1	0	rs145777339	P	0.0016
	exon26:c.6093T>C:p.S2031S	0	0	-	P	-
	exon22:c.3337G>C:p.D1113H	16	1	rs12713844	P	0.0067
	exon16:c.2258G>A:p.G753E	2	0	-	PP	0.0002
SCNN1B NM_000336	exon5:c.786G>A:p.T262T	0	0	rs150781093	P	0.000028
LDLR	exon7:r.spl	3	0	-	NA	-
NM_000527	exon10:c.1332C>T:p.A444A,	0	0	rs143872778	P	0.0002
	exon14:c.2140+5G>A	13	0	rs72658867	NA	0.0074

L, low; S, symptomatology; ICU, intensive care unit; AA, amino acid; US, uncertain significance, NA, not available; FH, familial hypercholesterolemia; P, polymorphism; PP, probable polymorphism; PHA, pseudohyperaldosteronism; BR, briochoectasis; SCL, sphingomyelin/cholesterol lipidosis; PYA, pseudohypoaldosteronism; Abeta, abetalipoproteinemia; Av SNP, average single nucleotide polymorphism.

The investigation of the patients in Group 2 of dyslipidemic patients revealed, as predicted, mutations in the genes *LDLR*, *MTTP*, *NOS2*, *FTO*, *APOB* and *AGTRI*, compatible with the underlying dyslipidemia.

In Group 3 of patients with L/NO S COVID-19, the variant NM_001038:exon2:c.112C>T:p.P38S was detected in the sodium channel epithelial 1 subunit α (*SCNN1A*) gene, which encodes the α subunit of the ENaC, with a minor allele frequency (Maf) <0.01, which is characterized as a variant of uncertain significance according to the National Center for Biotechnology Information (NCBI; https://www.ncbi.nlm.nih.gov/snp/rs3764873#clinical_significance).

In the COVID-19 Group 4 of patients with severe symptoms, the variant NM_000336:exon5:c.786G>A:p.T262T was detected in the *SCNN1B* gene, which encodes for the β subunit of ENaC, with a Maf <0.01 (Table III).

The P38S and T262T variants were further evaluated for their allele frequency in the in-house Exome Sequencing Database of the Laboratory of Medical Genetics of the St. Sophia's Children's Hospital, NKUA (Athens, Greece). Exome Sequencing (ES) data from 500 unrelated individuals, originally referred due to a clinically suspected genetic condition,

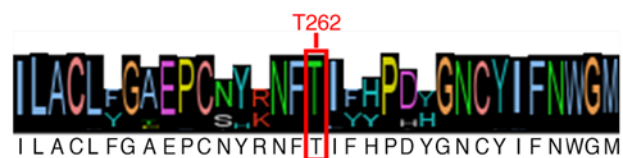


Figure 1. Logo representation of multiple sequence alignment of the sodium channel epithelial 1 subunit β protein and the conserved residue T262.

were also used. The cohort included a wide range of age groups, but 80% were children and adolescents up to the age of 18 years (12). Specifically, the allele frequency of these variants was evaluated in 500 randomly selected samples using the variant annotation and filter tool VarAFT (13,14).

The structure of the ENaC protein was retrieved by the Research Collaboratory for Structural Bioinformatics Protein Data Bank (ID no. 6WTH) at a resolution of 3.06 Å (15). An initial structural study was performed using the Molecular Operating Environment (MOE; version 2013.08; 2016; Chemical Computing Group Inc.; <https://www.chemcomp.com/en/Products.htm>) platform for the optimization of the three-dimensional protein structure and energy minimizations

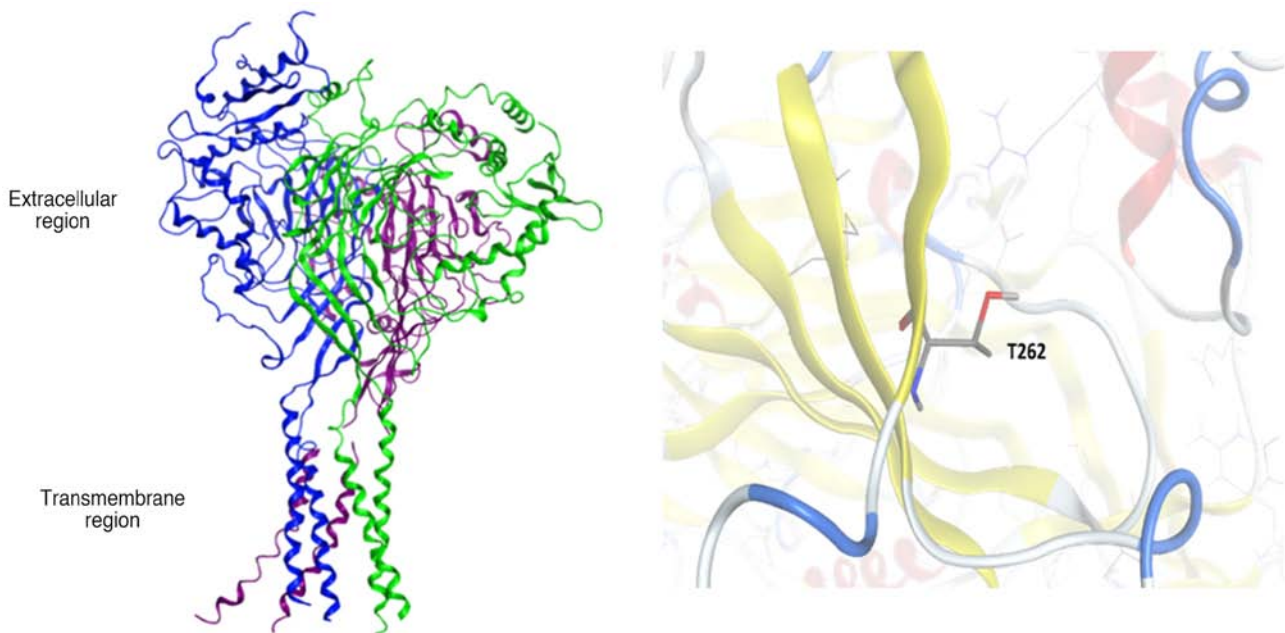


Figure 2. Left panel: The three-dimensional structure of epithelial sodium channel ENaC in cartoon representation assembled by the three subunits α (purple), β (blue) and γ (yellow), consisting of six helices that span the cell membrane and a large extracellular domain. Right panel: Threonine residue T262 of sodium channel epithelial 1 subunit β exposed on the surface.

and dynamic simulations under the CHARMM27 force field (16).

Amongst all retrieved sequences, the threonine residue in position 262 was 96.95% conserved (Fig. 1).

The human ENaC protein is comprised of the three subunits, α , β and γ . Each subunit consists of two transmembrane helices of 25-30 amino-acid length and a short intracellular region at the N- and C-terminus, whereas the large extracellular region of the protein encompasses multiple domains. Residue T262-SCNN1B is exposed on the extracellular space and no known mutations have been reported so far (Fig. 2).

The structural analysis of the SCNN1B protein in the present study revealed an overall rigid conformation. The crystallographic structure of the ENaC β subunit was fixed to remove geometric restraints using the 'Structure Preparation' module of the MOE platform. Energy minimization and molecular dynamic simulations resulted in a stable conformation with T262 located on the surface of the extracellular domain. In addition, computational mutation analysis in position 262 did not reveal any conformational changes in the overall structure.

Genetic networks and codon bias usage. The recovered genes were further analyzed for their ranking and function via GeneMania network (<http://www.genemania.org>). The constructed genetic network for SCNN1A and SCNN1B resulted in multiple interactions (Fig. 3). A total of 20 genes, including ENaC subunits α , β and γ , with-no-lysine kinases and serum and glucocorticoid-induced protein kinase, were revealed due to their physical interactions, i.e., the overall tertiary structure of ENaC, as well as the ENaC-specific kinases.

To explore codon usage bias in the identified SCNN1B variant, a statistical analysis was performed based on the

retrieved homologous sequences of SCNN1B. Multiple sequence alignments result in a 99.6% identity of threonine residues in position 262, and thus, a codon bias usage analysis was performed to calculate the frequency of threonine codon ACA against codon ACG. The analysis of the corresponding data for T262 codon usage of all the retrieved sequences revealed a high frequency of ~72,3% for the ACA codon and 12,1% for the ACG codon. The frequency of occurrence for the human ENaC- β subunit of the ACA and ACG codon for threonine was also calculated and was found to be 39 vs. 7%, respectively.

Discussion

Patients with SARS-CoV-2 infection may experience a wide range of clinical manifestations, from being asymptomatic to critical illness and even death. Several studies have suggested that variability in the genotype distribution of diverse gene polymorphisms may explain the variability in disease prevalence, morbidity and mortality of patients with COVID-19 among different regions of the world (17). In the current study, which aimed to identify a possible association of the genetic profile predisposing to cardiovascular diseases in patients with COVID-19, several findings have emerged: i) There was a positive genetic confirmation of inherited dyslipidemia in patients without COVID-19; ii) the ICU-COVID-19 participants exhibited significantly lower cholesterol levels; and iii) among all the observed variants in the present study, the rare variant P38S of the ENaC- α subunit in the group of patients with L/NO S COVID-19 and the rare variant T262T in the ENaC- β subunit were identified only in the ICU patients.

Lipid disorders may increase the risk of a severe course of COVID-19, but also the infection itself may alter the patient's metabolic profile, mainly by impairing the function

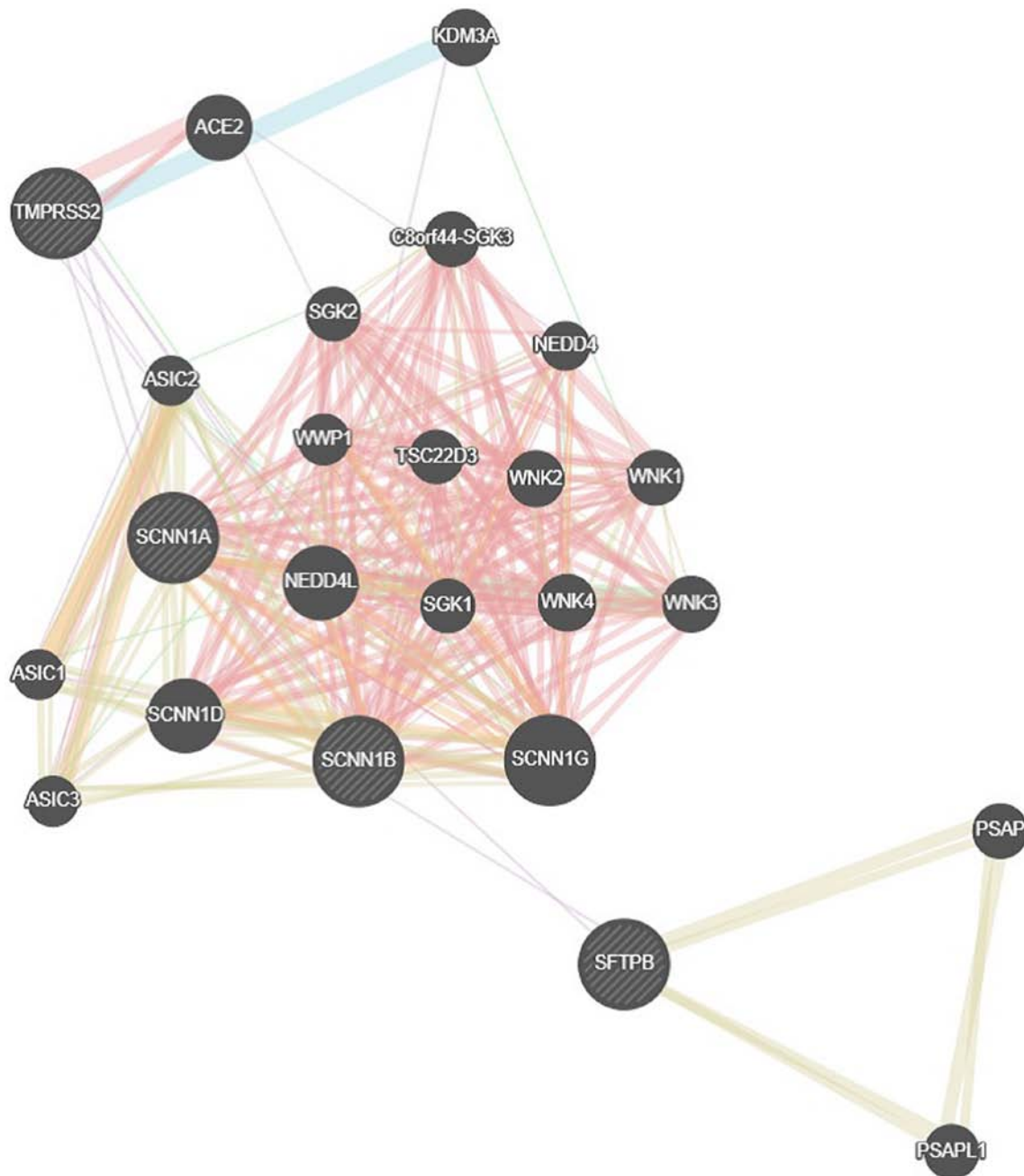


Figure 3. GeneMANIA genetic network for the SCNN1A-SCNN1B genes. SCNN1A, sodium channel epithelial 1 subunit α (related to the genes SCNN1G, SFTPB, ACE2, KDM3, TMPRSS2, ASIC1, ASIC2, ASIC3, SGK1, SGK2, C8ORF44, WWP1, NEDD4, NEDD4L, TSC22D3, WNK2, WNK1, WNK4, WNK3, PSAP and PSAPL1).

of HDLs (18). However, our genetically confirmed dyslipidemic patients appeared to not be vulnerable to severe or mild COVID-19 disease. Data from a study support the same impact of dyslipidemia in 5,279 patients. It was demonstrated that its occurrence was not associated with an increased risk of hospitalization ($P=0.51$) or mortality in patients with COVID-19 ($P=0.79$) (19). Similarly, another retrospective study of 211 patients failed to reveal any association of dyslipidemia with an increased risk of progression to severe COVID-19 disease ($P=0.940$) (20).

Another important observation was the low TC, LDL and HDL levels between patients in the ICU-COVID-19 and L/NO S groups (129.82 ± 28.33 vs. 215.38 ± 46.01 , $P<0.001$;

75.45 ± 23.14 vs. 133.46 ± 36.49 , $P<0.001$; and 33.00 ± 12.00 vs. 55.00 ± 10.00 , $P=0.001$). A recent prospective study of 108 patients with SARS-CoV-2, which evaluated their lipid profiles in a long-term follow-up, showed significantly lower TCs (140 vs. 175 mg/dl; $P<0.001$) and LDL cholesterol levels (71.3 vs. 98 mg/dl; $P=0.002$) (21).

Furthermore, in another observational cross-sectional study, which included 1,411 hospitalized patients with COVID-19, the usefulness of serum TC, LDL, non-HDL, HDL cholesterol and TGs in the prognosis was assessed. Similar to the present results, they observed that low HDL and high TGs before or during hospitalization were strong predictors of severe COVID-19. The researchers

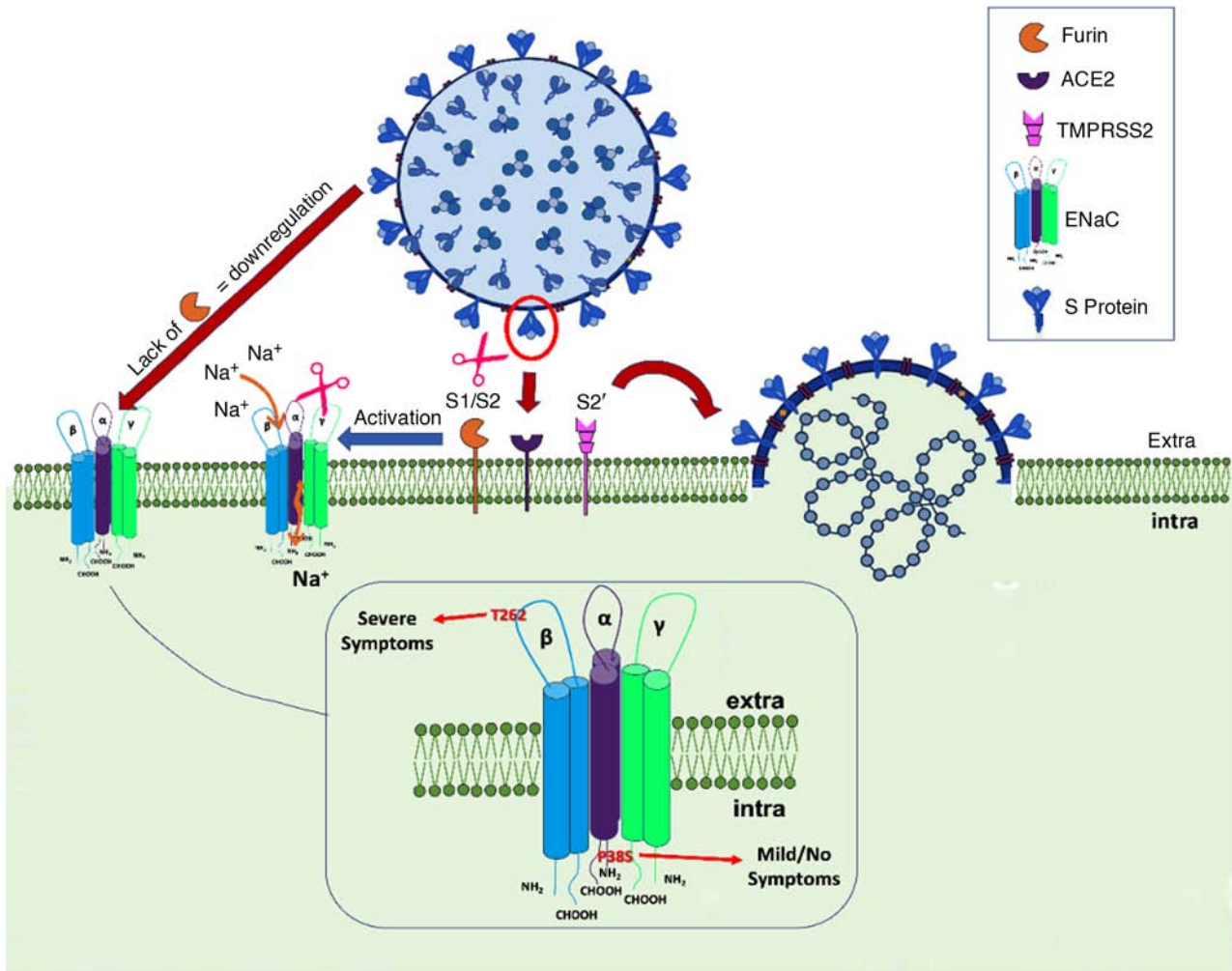


Figure 4. Potential role of ENaC in the pathogenesis of Coronavirus disease 2019. ENaC, epithelial sodium channel; S1, substrate 1; S protein, spike protein; $\alpha/\beta/\gamma$, alpha/beta/gamma subunits.

emphasized the notion that the lipid profile should be considered a sensitive marker of inflammation in patients with COVID-19. A possible explanation for the aforementioned outcomes is that patients with acute infections experience a hypercatabolic status combined with malnutrition; however, the contradiction of increased TG levels remains an issue (22).

The detected ENaC gene variants in the patients with COVID-19 were in two of the three homologous subunits (α , β and γ) of the heterotrimeric functional channels, which are selectively permeable to ions of sodium (Na^+) (23,24). These channels are constitutively active, allowing sodium reabsorption from the lumen into the apical cell membrane across epithelial cells, thus regulating the volume of the extracellular fluid and influencing arterial blood pressure. Aldosterone regulates their activity in the renal tubules and the distal colon, while atrial natriuretic peptide negatively modulates their function, leading to natriuresis and diuresis (25-30). Of note, ENaC channels are also expressed in the lingual epithelium and taste receptors, implicated in salt-taste perception and in non-epithelial cells, such as endothelial cells and vascular smooth muscle cells, where they act as mechanosensors (24,27,31).

Channels lacking the α subunit are completely nonfunctional, whereas channels lacking the β or γ subunits are hypofunctional (32). Human airways express a lesser-studied ENaC δ subunit, which is phylogenetically close to the ENaC- α subunit (33). Inactivating the α -ENaC subunit in mice leads to defective lung liquid clearance and premature death (34). Inactivating the β - and γ -subunits of ENaC also leads to early death in newborn mice due to fluid and electrolyte imbalances, suggesting that ENaC expression is critical for fetal lung fluid absorption.

Each of the ENaC subunits have a similar structure: A cytoplasmic N-terminus, an extracellular loop, two short hydrophobic segments (transmembrane domains 1 and 2) and a cytoplasmic C-terminus. The N- and C-termini are turned to the cytoplasmic surface, whereas the extracellular loop is turned to the extracellular space. The C-terminus of all ENaC subunits has a highly conserved sequence - the proline tyrosine motif (29). Cleavage of the extracellular domains renders ENaC constitutively active, whereas intracellular conditions and signaling involving the N- and C-termini of the ENaC subunits modulate the 'open' vs. 'closed' probability (P_o) of active channels (35). Point mutations at a highly conserved glycine residue in the N termini of any of the three subunits

markedly decrease the P_o via alterations in channel open and closed times (36).

Also, ENaC-mediated Na^+ conductance is controlled by internalization and proteasomal degradation following ubiquitination of the intracellular N-termini of the ENaC subunits (37). The latter process regulates the accessibility of cleavage sites in the extracellular domain to channel-activating proteases through conformational changes. Knight *et al* (38) demonstrated that intracellular sodium regulates the proteolytic activation of ENaC possibly by altering the accessibility of protease cleavage sites. Although these observations indicate that intracellular signaling or conditions can significantly influence extracellular cleavage and activation of ENaC, the molecular mechanism of such transmembrane allosteric regulation of ENaC remains elusive. The present observation of the N-terminal P38S may have a similar impact in decreasing the P_o affecting ENaC channel activity, whereas the extracellular T262T may have a regulatory role, given that extracellular domains of ENaC act as receptors for regulators controlling the activity of the channel (Fig. 4).

The expression and activity of ENaC are regulated by the RAAS member aldosterone and furin (37). SARS-CoV-2 spike protein harbors a furin cleavage site, which is similar to the ENaC furin-cleavable peptide. More specifically, the SARS-CoV-2 Spike (S) protein contains a putative furin recognition motif (680SPRRAR↓SV687) on the S1/S2 site, which is similar to the PRSVRSV motif of Middle Eastern respiratory syndrome coronavirus and serves as a protease recognition site. Similar sequence patterns have been identified in certain members of Alphacoronavirus, Betacoronavirus and Gammacoronavirus, whereas they are absent in Coronaviruses of zoonotic origin (Pangolin-CoV and Bat-CoV RaTG13) (39). This motif may represent an evolutionary advantage of SARS-CoV-2, facilitating its entry into host cells. Of note, when examining >10 million peptides of ~20,000 human proteins from UniProtKB, peptide PRRARSV is present solely in the human ENaC- α subunit. Proteolytic activation by the protease furin is a prerequisite for ENaC- α activation. However, proteolytic activation of S protein by cleavage at S1/S2 is also important for efficient viral entry into host target cells and plays a role in host species selectivity and infectivity (39,40). These findings suggest that SARS-CoV-2 has developed a mimicry mechanism of a human protease substrate of furin, thus hijacking protease pathways of ENaC- α for its activation in SARS-CoV-2-infected cells, compromising at the same time ENaC- α activation (41).

In addition, the present results showed that the ENaC- α gene is co-expressed with the transmembrane protease serine 2 (TMPRSS2) gene. ENaC- α exerts its function by binding to ACE2 and is recognized by TMPRSS2. The site at which TMPRSS2 cuts ENaC- α is identical to a small part of the SARS-CoV-2 S-protein. Given the high structural similarity between the S-protein and ENaC- α , neither ACE2 nor TMPRSS2 can discriminate between the virus and these molecules, allowing viral particles to enter host cells (41,42).

In the present study, it was also observed that ENaC- β is co-expressed and interacts genetically with NEDD4 like E3 ubiquitin protein ligase (NEDD4L). Nedd4L regulates the trafficking of membrane receptors, transporters and ion channels, such as the ENaC and as a member of HECT domain E3

ubiquitin protein ligase, has been implicated in the cell egress phase of certain RNA viruses, possibly high jacking the endosomal sorting complexes required for the transport known as ESCRT-0, ESCRT-I, ESCRT-II, and ESCRT-III. Together with a number of accessory proteins, these ESCRT complexes enable a unique mode of membrane remodeling that results in membranes bending/budding away from the cytoplasm. Novelli *et al* (43) identified the HECT family members of E3 ligases as likely novel biomarkers for COVID-19.

In addition, *SCNNIB* is co-expressed with the gene *NEDD4L*, which is involved in the regulation of insulin and insulin-like growth factor (IGF-1) signaling by regulating the amount of insulin receptor and IGF-1 receptor on the cell surface. The deletion of *NEDD4* in mice leads to a reduced number of effector T-cells and a slower T-cell response to antigens, suggesting that *NEDD4* may be implicated in the conversion of native T-cells into activated T-cells. Of note, both genes are co-expressed with the *SFTPB* gene, which encodes the pulmonary-associated surfactant B protein, an amphipathic surfactant protein essential for lung function and homeostasis. The latter genes encode the apolipoproteins that form ~8% of the surfactant fluid (consisting of surfactant protein A (SP-A; 5.5%, comprising of SP-A1 and SP-A2), SP-B (1%), SP-C (1%) and SP-D (0.5%)) (44). Pulmonary Surfactant Metabolism Dysfunction comprises a genetically heterogeneous group of disorders that result in severe respiratory insufficiency or failure in full-term neonates or infants. These disorders are associated with various pathologic entities, including pulmonary alveolar proteinosis, desquamative interstitial pneumonitis or cellular nonspecific interstitial pneumonitis. Thus, the co-expression of the *EaC- α* and *ENaC- β* genes with *SFTPB* may reveal the same transcriptional regulatory program, a functional relation and a common biological process (43,44).

The surface of SARS-CoV-2 viral bodies is covered by numerous glycosylated S proteins. These proteins bind to the membrane-bound ACE2 as a first step in the entry of viral particles into the host cell. Their entry into the cell depends on the cleavage of protein S (in Arg-667/Ser-668) by a serine protease. Anand *et al* (41) showed that this cleavage site has a sequence pattern that is homologous to the furin cleavage site in the ENaC channel. Gentzsch and Rossier (45) reported that the virus compromises the function of almost all organs by infecting the endothelium of blood vessels, where ENaC also plays an important role, causing inflammation and the release of cytokines (46).

As seen by the multiple sequence analysis, T262, as well as other amino acid residues in its proximity, are highly conserved (Fig. 1). In an effort to reveal a specific mechanism that may result in the association of the *SCNNIB* variant and the severe pathological phenotype in patients with SARS-CoV-2, a statistical analysis of the codon usage bias of this synonymous mutation was performed in the present study. The codons that correspond to the detected variant are ACA for 'wild-type' threonine and ACG for the 'mutated' threonine. The analysis of the corresponding data for T262 codon usage of all the retrieved sequences reveals a high frequency of ~72.3% for the ACA codon and 12.1% for the ACG codon. The frequency of occurrence for the human ENaC- β subunit of the ACA and ACG codon for threonine was also calculated and was found

to be 39 vs. 7%, respectively. At an intra-species level, codon usage for threonine in *Homo sapiens* corresponds to 15.1% (ACA) against 6.1% (ACG), also revealing the preference for ACA usage (47). Codon usage bias is well established and plays a crucial role in regulating gene expression. Not only synonymous codons and their corresponding tRNA availability are a way of fine-tuning the expression of genes; it has also been shown that synonymous codons cluster in the coding sequence, resulting in co-occurrence bias that mediates high expression levels.

The analysis of the ENaC structure and the SCNN1B T262T variant revealed a stable conformation of the extracellular domain and the neighboring region of T262 that is highly conserved. No structural feature was identified that could indicate a mechanism linked to SARS-CoV-2 infection, particularly for position 262. However, the codon usage bias for this synonymous mutation could point to a regulatory mechanism in terms of gene expression. The detected NM_000336:exon5:c.786G>A variant is most likely to result in a lack of tRNA availability for the alternative codon, leading to deficient SCNN1B expression.

In conclusion, a dysfunctional lipid profile due to the genetic phenotype or underlying diseases may be considered a prediction tool for COVID-19 severity. In addition, the identification of the two rare ENaC variants in ICU and L/NO S patients in the coding region may be predictive of whether the ENaC channel is involved in ENaC-mediated SARS-CoV-2 entry. Therefore, the effect of SARS-CoV-2 infection on ENaC function in different cells of the upper and lower respiratory tract and at different stages of the disease should be studied in a larger population to reinforce this hypothesis and further clarify its possible pathophysiological role in COVID-19 severity and progression.

Physicians should also be engaged in close monitoring of dyslipidemia patients with suspected COVID-19, for detecting signs of disease progression in a timely fashion. Finally, the presence of dyslipidemia may be an important factor in future risk stratification models for COVID-19.

Acknowledgements

Not applicable.

Funding

The authors gratefully acknowledge the financial support of Synenosis, Greek Shipowners' Social Welfare Company and especially the Angelakos Evangelos family.

Availability of data and materials

The data generated in the present study may be requested from the corresponding author (raw data are available at <http://www.ncbi.nlm.nih.gov/bioproject/1136239>).

Authors' contributions

EK, KH, AN, KG, DV, EP, NM, NR, SM and GPC conceived the study design and were involved in data interpretation. PB, AA, AtK and AnK, VE and JTS collected and analysed the data. GPC made critical revisions to the manuscript. EK and

GPC checked and confirmed the authenticity of the raw data. All authors read and approved the final manuscript.

Ethics approval and consent to participate

The study was approved by each Ethical Committee of the University Research Institute of Maternal and Child Health and Precision Medicine and UNESCO Chair on Adolescent Health Care and the National and Kapodistrian University of Athens and the ICU, First Department of Pulmonary Medicine, National and Kapodistrian University of Athens and Sotiria Hospital (Athens, Greece). All patients provided written informed consent to participate in this study according to the General Data Protection Regulation.

Patient consent for publication

Not applicable.

Competing interests

The authors declare that they have no competing interests.

References

- Huang C, Wang Y, Li X, Ren L, Zhao J, Hu Y, Zhang L, Fan G, Xu J, Gu X, *et al*: Clinical features of patients infected with 2019 novel coronavirus in Wuhan, China. *Lancet* 395: 497-506, 2020.
- Wang D, Hu B, Hu C, Zhu F, Liu X, Zhang J, Wang B, Xiang H, Cheng Z, Xiong Y, *et al*: Clinical characteristics of 138 hospitalized patients with 2019 novel coronavirus-infected pneumonia in Wuhan, China. *JAMA* 323: 1061-1069, 2020.
- Tall AR and Yvan-Charvet L: Cholesterol, inflammation and innate immunity. *Nat Rev Immunol* 15: 104-116, 2015.
- Soy M, Keser G, Atagündüz P, Tabak F, Atagündüz I and Kayhan S: Cytokine storm in COVID-19: Pathogenesis and overview of anti-inflammatory agents used in treatment. *Clin Rheumatol* 39: 2085-2094, 2020.
- Kaji H: High-density lipoproteins and the immune system. *J Lipids* 2013: 684903, 2013.
- McKechnie JL and Blish CA: The innate immune system: Fighting on the front lines or fanning the flames of COVID-19? *Cell Host Microbe* 27: 863-869, 2020.
- Kim JA, Montagnani M, Chandrasekran S and Quon MJ: Role of lipotoxicity in endothelial dysfunction. *Heart Fail Clin* 8: 589-607, 2012.
- Froldi G and Dorigo P: Endothelial dysfunction in Coronavirus disease 2019 (COVID-19): Gender and age influences. *Med Hypotheses* 144: 110015, 2020.
- Kim D, Chung H, Lee JE, Kim J, Hwang J and Chung Y: Immunologic aspects of dyslipidemia: A critical regulator of adaptive immunity and immune disorders. *J Lipid Atheroscler* 10: 184-201, 2021.
- Lei P, Zhang L, Han P, Zheng C, Tong Q, Shang H, Yang F, Hu Y, Li X and Song Y: Liver injury in patients with COVID-19: Clinical profiles, CT findings, the correlation of the severity with liver injury. *Hepatol Int* 14: 733-742, 2020.
- Malik J, Laique T, Ishaq U, Ashraf A, Malik A, Ali M, Zaidi SMJ, Javaid M and Mehmood A: Effect of COVID-19 on lipid profile and its correlation with acute phase reactants. *medRxiv*: doi: <https://doi.org/10.1101>.
- Marinakos NM, Svingou M, Veltra D, Kekou K, Sofocleous C, Tilemis FN, Kosma K, Tsoutsou E, Fryssira H and Traeger-Synodinos J: Phenotype-driven variant filtration strategy in exome sequencing toward a high diagnostic yield and identification of 85 novel variants in 400 patients with rare Mendelian disorders. *Am J Med Genet A* 185: 2561-2571, 2021.
- Tilemis FN, Marinakis NM, Veltra D, Svingou M, Kekou K, Mitrakos A, Tzetis M, Kosma K, Makrythanasis P, Traeger-Synodinos J and Sofocleous C: Germline CNV detection through whole-exome sequencing (WES) data analysis enhances resolution of rare genetic diseases. *Genes (Basel)* 14: 1490, 2023.

14. Desvignes JP, Bartoli M, Delague V, Krahn M, Miltgen M, Bérout C and Salgado D: VarAFT: A variant annotation and filtration system for human next generation sequencing data. *Nucleic Acids Res* 46 (W1): W545-W553, 2018.
15. Noreng S, Posert R, Bharadwaj A, Houser A and Bacongus I: Molecular principles of assembly, activation, and inhibition in epithelial sodium channel. *Elife* 9: e59038, 2020.
16. Foloppe N and MacKerell AD Jr: All-Atom empirical force field for nucleic Acids: 2) parameter optimization based on small molecule and condensed phase macromolecular target data. *J Comput Chem* 21: 86-104, 2000.
17. Yamamoto T, Uchiumi C, Suzuki N, Yoshimoto J and Murillo-Rodriguez E: The psychological impact of 'mild lockdown' in Japan during the COVID-19 pandemic: A nationwide survey under a declared state of emergency. *Int J Environ Res Public Health* 7: 9382, 2020.
18. Li H, Xiang X, Ren H, Xu L, Zhao L, Chen X, Long H, Wang Q and Wu Q: Serum amyloid A is a biomarker of severe coronavirus disease and poor prognosis. *J Infect* 80: 646-655, 2020.
19. Petrilli CM, Jones SA, Yang J, Rajagopalan H, O'Donnell L, Chernyak Y, Tobin KA, Cerfolio RJ, Francois F and Horwitz LI: Factors associated with hospital admission and critical illness among 5279 people with coronavirus disease 2019 in New York City: Prospective cohort study. *BMJ* 369: m1966, 2020.
20. Chang MC, Park YK, Kim BO and Park D: Risk factors for disease progression in COVID-19 patients. *BMC Infect Dis* 20: 445, 2020.
21. Aparisi A, Martín-Fernández M, Ybarra-Falcón C, Gil J, Carrasco-Moraleja M, Martínez-Paz P, Cusacovich I, Gonzal-Benito H, Fuertes R, Marcos-Mangas M, *et al*: Dyslipidemia and Inflammation as Hallmarks of oxidative stress in COVID-19: A follow up study. *Int J Mol Sci* 23: 15350, 2022.
22. Masana L, Correig E, Ibarretxe D, Anoro E, Arroyo JA, Jericó C, Guerrero C, Miret M, Naf S, Pardo A, *et al*: Low HDL and high triglycerides predict COVID-19 severity. *Sci Rep* 11: 7217, 2021.
23. Mano I and Driscoll M: DEG/ENaC channels: A touchy superfamily that watches its salt. *Bioessays* 21: 568-578, 1999.
24. Drummond HA, Grifoni SC and Jernigan NL: A New Trick for an Old Dogma: ENaC proteins as mechanotransducers in vascular smooth muscle. *Physiology* (Bethesda) 23: 23-31, 2008.
25. Govindan R, Banerjee P, Dhania NK and Senapati S: FTIR based approach to study EnaC mechanosensory functions. *Prog Biophys Mol Biol* 167: 79-86, 2021.
26. Kashlan OB and Kleyman TR: ENaC structure and function in the wake of a resolved structure of a family member. *Am J Physiol Renal Physiol* 301: F684-F696, 2011.
27. Baldin JP, Barth D and Fronius M: Epithelial Na⁺ channel (ENaC) formed by one or two subunits forms functional channels that respond to shear force. *Front Physiol* 11: 141, 2020.
28. Champigny G, Voilley N, Lingueglia E, Friend V, Barbry P and Lazdunski M: Regulation of expression of the lung amiloride-sensitive Na⁺ channel by steroid hormones. *EMBO J* 13: 2177-2181, 1994.
29. Hanukoglu I and Hanukoglu A: Epithelial sodium channel (ENaC) family: Phylogeny, structure-function, tissue distribution, and associated inherited diseases. *Gene* 579: 95-132, 2016.
30. Kellenberger S and Schild L: International Union of Basic and Clinical Pharmacology. XCI. structure, function, and pharmacology of acid-sensing ion channels and the epithelial Na⁺ Channel. *Pharmacol Rev* 67: 1-35, 2015.
31. Golestaneh N, Klein C, Valamanesh F, Suarez G, Agarwal MK and Mirshahi M: Mineralocorticoid receptor-mediated signaling regulates the ion gated sodium channel in vascular endothelial cells and requires an intact cytoskeleton. *Biochem Biophys Res Commun* 280: 1300-1306, 2001.
32. Canessa CM, Schild L, Buell G, Thorens B, Gautschi I, Horisberger JD and Rossier BC: Amiloride-sensitive epithelial Na⁺ channel is made of three homologous subunits. *Nature* 367: 463-467, 1994.
33. Waldmann R, Champigny G, Bassilana F, Voilley N and Lazdunski M: Molecular cloning and functional expression of a novel amiloride-sensitive Na⁺ channel. *J Biol Chem* 270: 27411-27414, 1995.
34. Hummler E, Barker P, Gatzky J, Beermann F, Verdumo C, Schmidt A, Boucher R and Rossier BC: Early death due to defective neonatal lung liquid clearance in alpha-ENaC-deficient mice. *Nat Genet* 12: 325-328, 1996.
35. Tong Q, Gamper N, Medina JL, Shapiro MS and Stockand JD: Direct activation of the epithelial Na⁺(+) channel by phosphatidylinositol 3,4,5-trisphosphate and phosphatidylinositol 3,4-bisphosphate produced by phosphoinositide 3-OH kinase. *J Biol Chem* 279: 22654-22663, 2004.
36. Gründer S, Firsov D, Chang SS, Jaeger NF, Gautschi I, Schild L, Lifton RP and Rossier BC: A mutation causing pseudohypoaldosteronism type 1 identifies a conserved glycine that is involved in the gating of the epithelial sodium channel. *EMBO J* 16: 899-907, 1997.
37. Ruffieux-Daidié D, Poirot O, Boulkroun S, Verrey F, Kellenberger S and Staub O: Deubiquitylation regulates activation and proteolytic cleavage of ENaC. *J Am Soc Nephrol* 19: 2170-2180, 2008.
38. Knight KK, Wentzlaff DM and Snyder PM: Intracellular sodium regulates proteolytic activation of the epithelial sodium channel. *J Biol Chem* 283: 27477-27482, 2008.
39. Örd M, Faustova I and Loog M: The sequence at Spike S1/S2 site enables cleavage by furin and phospho-regulation in SARS-CoV2 but not in SARS-CoV1 or MERS-CoV. *Sci Rep* 10: 16944, 2020.
40. Bonny O and Hummler E: Dysfunction of epithelial sodium transport: From human to mouse. *Kidney Int* 57: 1313-1318, 2000.
41. Anand P, Puranik A, Aravamudan M, Venkatakrishnan AJ and Soundararajan V: SARS-CoV-2 strategically mimics proteolytic activation of human ENaC. *Elife* 9: e58603, 2020.
42. V'kovski P, Kratzel A, Steiner S, Stalder H and Thiel V: Coronavirus biology and replication: Implications for SARS-CoV-2. *Nat Rev Microbiol* 19: 155-170, 2021.
43. Novelli G, Biancolella M, Mehrian-Shai R, Colona VL, Brito AF, Grubaugh ND, Vasiliou V, Luzzatto L and Reichardt JKV: COVID-19 one year into the pandemic: From genetics and genomics to therapy, vaccination, and policy. *Hum Genomics* 15: 27, 2021.
44. Gandhi CK, Chen C, Wu R, Yang L, Thorenoor N, Thomas NJ, DiAngelo SL, Spear D, Keim G, Yehya N and Floros J: Association of SNP-SNP interactions of surfactant protein genes with pediatric acute respiratory failure. *J Clin Med* 9: 1183, 2020.
45. Gentzsch M and Rossier BC: A pathophysiological model for COVID-19: Critical importance of transepithelial sodium transport upon airway infection. *Function (Oxf)* 1: zqaa024, 2020.
46. Ji HL, Song W, Gao Z, Su XF, Nie HG, Jiang Y, Peng JB, He YX, Liao Y, Zhou YJ, *et al*: SARS-CoV proteins decrease levels and activity of human ENaC via activation of distinct PKC isoforms. *Am J Physiol Lung Cell Mol Physiol* 296: L372-L383, 2009.
47. Quax TE, Claassens NJ, Söll D and van der Oost J: Codon bias as a means to fine-tune gene expression. *Mol Cell* 59: 149-161, 2015.

